

Electrodeposition of Magnetite on Carbon Steel in Fe(III)-Triethanolamine Solution and Its Corrosion Behavior

Soon-Hyeok Jeon, Geun-Dong Song and Do-Haeng Hur*

Nuclear Materials Safety Research Division, Korea Atomic Energy Research Institute,
989-111 Daedeok-daero, Yuseong-gu, Daejeon 305-353, Republic of Korea

A dense and adhesive magnetite layer was successfully electrodeposited on a carbon steel in the Fe(III)-TEA solution. Electrochemical tests for the carbon steel and magnetite were conducted in an alkaline solution. These tests using the adherent magnetite specimens produced by electrodeposition is a new method to investigate the corrosion behavior of magnetite. The corrosion resistance of magnetite is superior to that of the carbon steel. When the magnetite and carbon steel are electrically contacted, the magnetite and carbon steel play the role of cathode and anode because the corrosion potential of the magnetite was higher than that of the carbon steel. If the magnetite and carbon steel are galvanically contacted to the equivalent area ratio (1 : 1), the corrosion rate of galvanic coupled carbon steel will increase by about 3.5 times than that of non-coupled carbon steel. [doi:10.2320/matertrans.M2015016]

(Received January 7, 2015; Accepted April 14, 2015; Published May 29, 2015)

Keywords: electrodeposition, carbon steel, galvanic corrosion, magnetite

1. Introduction

Magnetite is the main corrosion product formed on the surface of carbon steel especially in secondary system of pressurized water reactor. This corrosion product reduces the efficiency of the steam generator by deterioration of the heat transfer and cause an acceleration of the corrosion of steam generator tube.¹⁻³⁾ Hence, its removal improves heat transfer and reduces localized corrosion.¹⁾

Some authors recently presented that the magnetite accelerates the corrosion of the carbon steel by a galvanic coupling.^{4,5)} Fushimi *et al.*⁴⁾ showed that the hydrogen generation on the single crystal magnetite as well as the reduction of the magnetite was contributed to a galvanic corrosion of the carbon steel in sulfate solutions. Al-Mayouf⁵⁾ presented that the galvanic coupling between magnetite and iron accelerated the corrosion of iron due to the small shift in potential of iron in the anodic direction in an acid solution. However, there is no investigation related to the corrosion behavior of a galvanic couple between carbon steel and proper magnetite in the simulated secondary water of pressurized water reactors.

In order to elucidate the corrosion behavior of carbon steel galvanically coupled with magnetite, it is necessary to use a proper magnetite specimen. Recently, it has been investigated that methods to produce a magnetite layer by electrodeposition.⁶⁻¹⁰⁾ Magnetite layer was electrodeposited in various solutions by oxidation of Fe(II)⁶⁻⁸⁾ or reduction of Fe(III)^{9,10)} on the electrode surface through a chemical reaction between the generated species and the original cations. Sapijeszko and Matijevic¹¹⁾ developed the hydrothermal method to produce the magnetite powder in Fe(III)-triethanolamine (TEA) solution at 523 K. Recently, Kothari *et al.*¹²⁾ have modified the Fe(III)-TEA solution and shown that magnetite is produced by electrodeposition on the stainless steel substrate at 333–363 K. However, there are few studies on the electrochemical behavior of magnetite

using the magnetite specimens manufactured by electrodeposition in the Fe(III)-TEA solution.

In this work, magnetite was deposited on the carbon steel substrate by electrodeposition in the Fe(III)-TEA solution. The electrochemical parameters of carbon steel and electrodeposited magnetite were measured in an alkaline solution by potentiodynamic tests for the first time. Electrochemical tests using the adherent magnetite specimens produced by electrodeposition is a new method to study the electrochemical behavior of magnetite. In consideration of the various applications, it is certainly worthwhile if this electrodeposited magnetite specimens are apply to the electrochemical tests.

2. Experimental

Carbon steel specimens for magnetite deposition were machined into 10 mm × 5 mm × 2 mm from the SA106Gr.B pipe material. The carbon steel substrates were mechanically ground up to #1000 grit silicon carbide paper and then ultrasonically cleaned in acetone and deionized water. Chemical compositions of carbon steel were presented in Table 1.

Magnetite were electrodeposited in Fe₂(SO₄)₃ solution complexed with TEA. The deposition bath for magnetite was prepared by dissolving 2.6 g of Fe(III) sulfate hydrate in 15 mL of 1 M TEA, resulting in a deep red colored solution. It was diluted with 50 mL of deionized water. The solution was then added to a second solution of 12.0 g of NaOH pellets in 85 mL of deionized water. The resulting gray-green solution was heated to 353 K and stirred at 200 rpm. The electrochemical deposition was carried out in a three electrode cell. A saturated calomel electrode (SCE) and a platinum wire were used as the reference and counter electrode, respectively.

After deposition, the magnetite was analyzed using scanning electron microscope-energy dispersive X-ray spectroscopy (SEM-EDS) and X-ray diffraction (XRD). The electrodeposited magnetite on the carbon steel substrate was milled by a focused ion beam (FIB) toward a vertical

*Corresponding author, E-mail: dhhur@kaeri.re.kr

Table 1 Chemical compositions of the carbon steel (mass%).

C	Cr	Ni	Mo	Si	Cu	Mn	S	P	Fe
0.19	0.4	0.2	0.1	0.23	0.1	1.05	0.005	0.012	Bal.

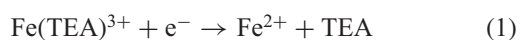
direction of the magnetite. Then, the morphology, thickness and chemical composition of the magnetite were analyzed.

The electrochemical corrosion tests were conducted in deaerated solution at 298 K. A saturated calomel electrode (SCE) and a platinum wire were used as the reference and counter electrode, respectively. The pH of the test solution was adjusted to be 9.5 with ethanolamine (ETA), which is used as a major organic reagent to control the pH of secondary water in nuclear power plants. The solution was deaerated by blowing a high purity nitrogen gas at a rate of $600 \text{ cc} \cdot \text{min}^{-1}$ during the tests. After the open circuit potential (OCP) was stabilized, polarization scan was started from the OCP to the cathodic or anodic direction with a scan rate of $1 \times 10^{-3} \text{ V} \cdot \text{s}^{-1}$. Therefore, each cathodic and anodic polarization curve was obtained from a newly prepared sample. The corrosion current density (i_{corr}) was commonly obtained by the extrapolation of the cathodic and anodic curve between 50 and 100 mV away from the corrosion potential (E_{corr}). The potentiodynamic polarization tests were conducted at least three times per specimen for reproducibility and reliability. Good reproducibility was confirmed.

3. Results and Discussion

3.1 Electrodeposition of the magnetite

Figure 1 shows linear sweep voltammogram on the carbon steel substrate in the Fe(III)-TEA bath at 353 K. The potential was swept from the OCP to $-1.30 \text{ V}_{\text{SCE}}$ at a scan rate of $5 \times 10^{-3} \text{ V} \cdot \text{s}^{-1}$. The electrochemical reduction of Fe(III)-TEA was observed at the more negative potential than approximately $-0.95 \text{ V}_{\text{SCE}}$. Increasing cathodic current density corresponding to the magnetite deposition started at $-0.95 \text{ V}_{\text{SCE}}$. The first reduction wave of this linear sweep, measured approximately between -0.95 and $-1.25 \text{ V}_{\text{SCE}}$, shows a one electron reaction corresponding to eq. (1).^{12,13} During the initial stage of electrodeposition at $-1.05 \text{ V}_{\text{SCE}}$, increase of the surface area by deposition of magnetite slightly increased the cathodic current density due to the increase of the current. Between -1.25 and $-1.30 \text{ V}_{\text{SCE}}$, a two-electron process shows the reduction of Fe(II) to Fe then for more negative potential the increase of the cathodic current density was due to hydrogen gas evolution corresponding to eq. (2).^{13,14} The current density was an about $-5.2 \text{ mA}/\text{cm}^2$ at the end of first wave, whereas it was about $-58 \text{ mA}/\text{cm}^2$ for the second wave at $-1.30 \text{ V}_{\text{SCE}}$.



Electrochemical studies using cyclic voltammetry have shown that the reduction of Fe(III)-TEA complexes is a one electron process in which an Fe(III)-TEA complex is reduced to an Fe(II)-TEA complex.¹⁵ The electrodeposition of magnetite film in a Fe(III)-TEA complexes can be simplified

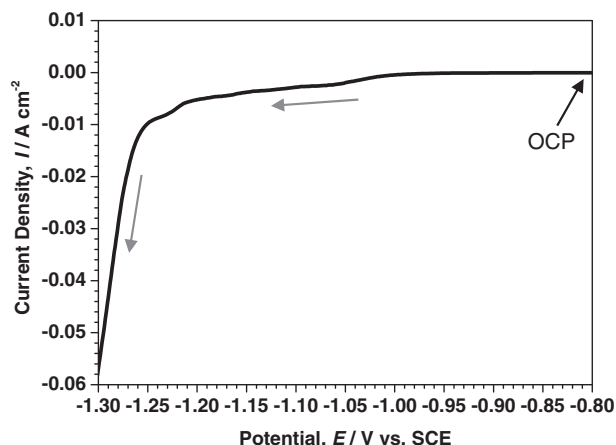


Fig. 1 Linear sweep voltammogram of carbon steel in the Fe(III)-TEA solution at 353 K.

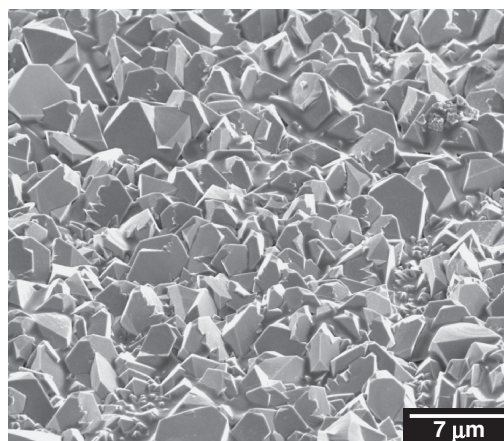
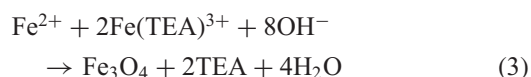


Fig. 2 SEM image of magnetite electrodeposited on the carbon steel substrate at the applied potential of $-1.05 \text{ V}_{\text{SCE}}$ in the Fe(III)-TEA solution at 353 K.

by two steps. First step is that the Fe(III)-TEA complex is electrochemically reduced to Fe^{2+} and TEA and second step is that the electrochemically produced Fe^{2+} next reacts chemically with Fe(III)-TEA complex in solution to produce magnetite film. The proposed mechanism is expressed in eqs. (1) and (3) as follows.¹²⁻¹⁴



In this work, magnetite was electrodeposited on the carbon steel substrate in the Fe(III)-TEA solution at 353 K. The magnetite was deposited at the potential of $-1.05 \text{ V}_{\text{SCE}}$ (first reduction wave region) for 1800 s. Figure 2 shows a SEM image of the magnetite electrodeposited on the carbon steel substrate. The magnetite has highly faceted and dense morphologies. This morphology is homogeneous on the whole surface of the deposit. Figure 3 shows the XRD analysis of the magnetite electrodeposited on the carbon steel substrate. This morphology is homogeneous on the whole surface of the deposit. The magnetite is all crystalline, and only has peaks corresponding to magnetite.

Figure 4 presents the SEM-EDS analysis of cross sectional electrodeposited magnetite films on the carbon steel sub-

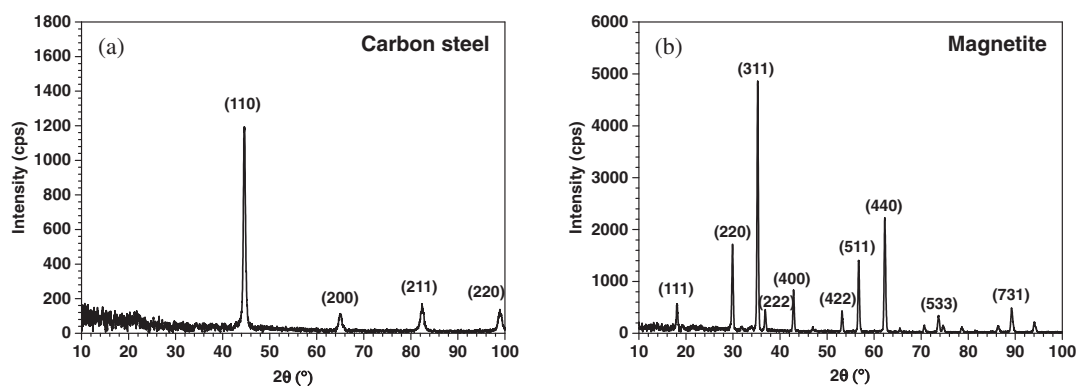


Fig. 3 XRD analysis of the carbon steel and electrodeposited magnetite on the carbon steel substrate at the applied potential of $-1.05 V_{SCE}$ in the Fe(III)-TEA solution at 353 K: (a) carbon steel and (b) electrodeposited magnetite.

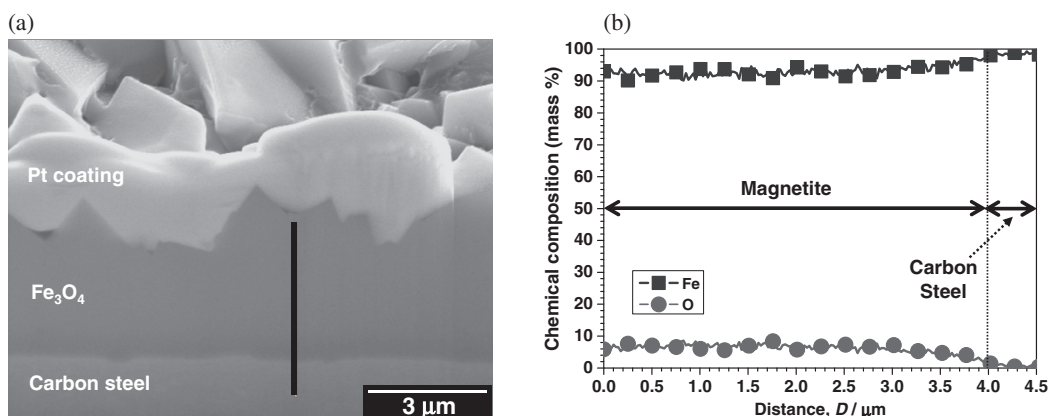


Fig. 4 SEM-EDS analysis of magnetite electrodeposited on the carbon steel substrate at the applied potential of $-1.05 V_{SCE}$ in the Fe(III)-TEA solution at 353 K: (a) cross section of magnetite and (b) line analysis.

strate. The thickness of the magnetite was ranged from 2.7 to $4.4 \mu\text{m}$, with an average of $3.5 \mu\text{m}$. Adherent magnetite deposited on carbon steel substrate is shown in Fig. 4(a). No gap or hole can be observed at the interface between magnetite and carbon steel substrate, which confirms that magnetite tightly bonded to carbon steel substrate. Line analysis of the magnetite is presented in Fig. 4(b). Content of oxygen was presented mainly in magnetite, and then the content of oxygen decrease from magnetite to carbon steel substrate. Iron content was presented mainly in carbon steel, and then the content of iron decrease from carbon steel substrate to magnetite.

3.2 Electrochemical behavior of the magnetite and carbon steel

Figure 5 shows the OCP curves of electrodeposited magnetite and carbon steel in an alkaline solution with pH 9.5 at 298 K as a function of time. The OCP of the magnetite was higher than that of the carbon steel.

Figure 6 shows the potentiodynamic polarization curves of the electrodeposited magnetite and carbon steel in an alkaline solution with pH 9.5 at 298 K. Using the newly prepared two samples, polarization scan was started from the OCP to the cathodic or anodic direction after the OCP was stabilized. In order to confirm the reproducibility, the potentiodynamic polarization tests were conducted at least three times on each specimen. The E_{corr} ($-0.420 V_{SCE}$) of the magnetite was

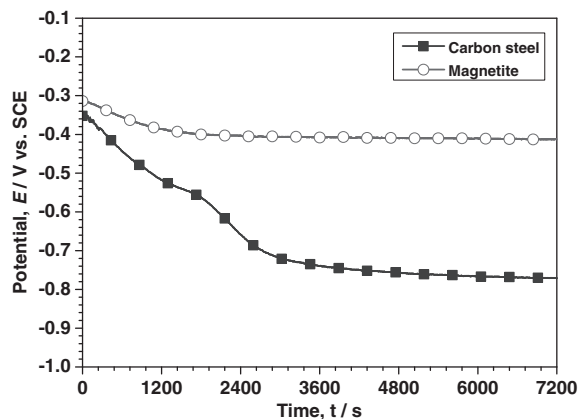
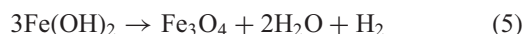
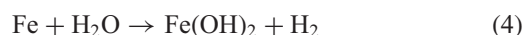


Fig. 5 Open circuit potential curves of electrodeposited magnetite and carbon steel in the alkaline solution at 298 K.

higher than that ($-0.780 V_{SCE}$) of the carbon steel. The i_{corr} ($1.04 \mu\text{A}/\text{cm}^2$) of magnetite is lower than that ($2.65 \mu\text{A}/\text{cm}^2$) of carbon steel. Based on the E_{corr} and i_{corr} , the corrosion resistance of magnetite is superior to that of the carbon steel. In anodic reaction, magnetite layer was formed on the carbon steel according to eqs. (4) and (5) as follows.^{16,17)}



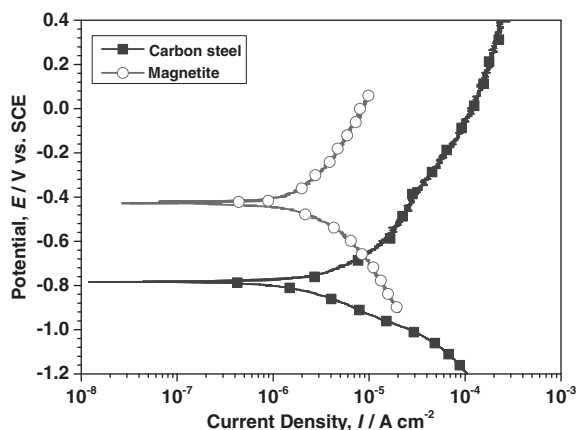
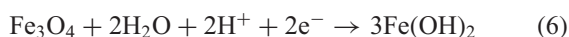


Fig. 6 Potentiodynamic polarization curves of electrodeposited magnetite and carbon steel in the alkaline solution at 298 K.

In cathodic reaction, the reductive dissolution of magnetite and formation of dissolved ferrous or ferrous species were occurred according to eq. (6) as the follows.^{18,19)} Some authors presented that the reductive dissolution of magnetite is occurred in the alkalized reducing condition.¹⁸⁾



When the magnetite and carbon steel are electrically contacted, the magnetite and carbon steel play the role of cathode and anode, respectively, because the E_{corr} of the magnetite was higher than that of the carbon steel. If the magnetite and carbon steel are galvanically contacted to the equivalent area ratio (1 : 1), the corrosion rate of galvanic coupled carbon steel will increase by about 3.5 times than that of non-coupled carbon steel. The galvanic coupling accelerates the corrosion of carbon steel based on the mixed potential theory.^{20,21)} The intersection point of the cathodic curve of magnetite and the anodic curve of carbon steel is the coupled potential ($E_{\text{couple}} = -0.66 \text{ V}_{\text{SCE}}$) of the galvanic coupling. The current density ($i_{\text{couple}} = 9.38 \mu\text{A}/\text{cm}^2$) of galvanic coupled carbon steel is higher than the i_{corr} of the non-coupled carbon steel. The corrosion behavior of carbon steel galvanically coupled with magnetite is schematically presented in Fig. 7.

The same phenomenon is also expected to occur in the area of spallation and turbulence. A repeated generation and collapse of bubbles can occur in the area immediately downstream of an orifice where the local static pressure of flowing water drops below the vapor pressure.²²⁾ When the magnetite layer is destroyed by cavitation, therefore, the bare surface of carbon steel is exposed to the flowing water. In addition, flow accelerated corrosion is most severe in the regions such as elbows, tees and bends where the pattern of the turbulent flow changes. These areas are expected to contain very little magnetite remaining on the surface, and expose the bare surface of carbon steel. This means that the local areas are in the condition of an unfavorably large ratio of the cathodic to anodic area. Therefore, corrosion rate of carbon steel is accelerated by a galvanic corrosion process.

4. Conclusions

A dense and adhesive magnetite layer was successfully

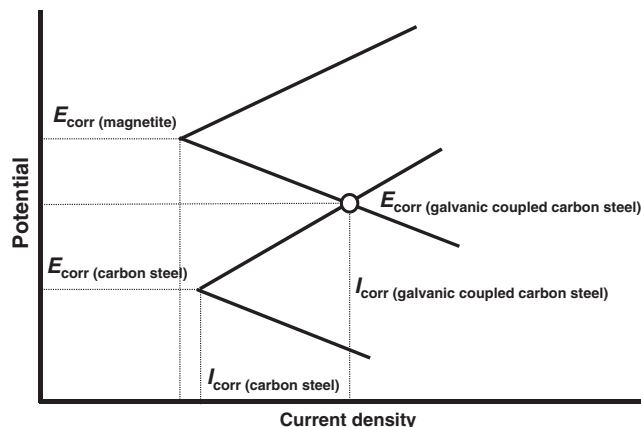


Fig. 7 Schematic of corrosion behavior of carbon steel galvanically coupled with magnetite in the alkaline solution.

electrodeposited on a carbon steel in the Fe(III)-TEA solution at 353 K. Electrochemical tests using the adherent magnetite specimens produced by electrodeposition is a new method to investigate the corrosion behavior of magnetite.

Based on the E_{corr} and i_{corr} , the corrosion resistance of magnetite is superior to that of the carbon steel. When the magnetite and carbon steel are electrically contacted, the magnetite and carbon steel play the role of cathode and anode. If the magnetite and carbon steel are galvanically contacted to the equivalent area ratio (1 : 1), the corrosion rate of galvanic coupled carbon steel will increase by about 3.5 times than that of non-coupled carbon steel.

Acknowledgements

This work was supported by the Nuclear Power Core Technology Development Program of the Korea Institute of Energy Technology Evaluation and Planning (KETEP) granted financial resource from the Ministry of Trade, Industry & Energy, Republic of Korea (2013T100100029).

REFERENCES

- 1) I. H. Plonski: *J. Appl. Electrochem.* **27** (1997) 1184.
- 2) C. Ramesh, N. Murugesan, A. A. M. Prince, S. Velmurugan, S. V. Narasimhan and V. Ganesan: *Corros. Sci.* **43** (2001) 1865.
- 3) A. A. M. Prince, S. Velmurugan, S. V. Narasimhan, C. Ramesh, N. Murugesan, P. S. Raghavan and R. J. Gopalan: *Nucl. Mater.* **289** (2001) 281.
- 4) K. Fushimi, T. Yamamuro and M. Seo: *Corros. Sci.* **44** (2002) 611.
- 5) A. M. Al-Mayouf: *Corros. Sci.* **48** (2006) 898.
- 6) D. Carlier, C. Terrier, C. Arm and J. P. Anserment: *Electrochim. Solid State Lett.* **8** (2005) 43.
- 7) S. Peulon, H. Antony, L. Legrand and A. Chausse: *Electrochim. Acta* **49** (2004) 2891.
- 8) S. Y. Wang, K. C. Ho, S. L. Kuo and N. L. Wu: *Electrochem. Soc.* **153** (2006) 75.
- 9) C. L. Teng and M. P. Ryan: *Electrochim. Solid State Lett.* **10** (2007) 108.
- 10) S. Mitra, P. Poizot, A. Finke and J. M. Tarascon: *Adv. Funct. Mater.* **16** (2006) 2281.
- 11) R. S. Sapieszko and E. Matijevic: *J. Colloids Interface Sci.* **74** (1980) 405.
- 12) H. M. Kothari, E. A. Kulp, S. J. Limmer, P. Poizot, E. W. Bohannon and J. A. Switzer: *J. Mater. Res.* **21** (2006) 293.
- 13) E. A. Kulp, H. M. Kothari, S. J. Limmer, J. Yang, R. V. Gudavarthy, E. W. Bohannon and J. A. Switzer: *Chem. Mater.* **21** (2009) 5022.

- 14) C. Goujon, T. Pauporte, C. Mansour, S. Delaunary and J. L. Bretelle: Proc. Int. Conference on Heat Exchanger Fouling and Cleaning, Budapest, Hungary, (2013) p. 101.
- 15) S. Mohr and T. Bechtold: *J. Appl. Electrochem.* **31** (2001) 363.
- 16) T. M. Laronge and M. A. Ward: NACE international, Corrosion 99, (1999) Paper No 345.
- 17) J. O. Bobinson and T. Drews: NACE international, Corrosion 99, (1999) Paper No 346.
- 18) K. S. Jung and K. W. Sung: *Magnetite: Structure, Properties and Applications*, (Nova Science Publishers, New York, 2010) pp. 261–298.
- 19) M. Vepsäläinen and T. Saario: VTT-R-09735-10, (2010).
- 20) K. D. Eiford: *STP 978 Galvanic corrosion* ed. by H. P. Hack, Philadelphia, (American Society for Testing and Materials 1988) p. 260.
- 21) J. W. Oldfield: *STP 978 Galvanic corrosion* ed. by H. P. Hack, Philadelphia, (American Society for Testing and Materials 1988). p. 5.
- 22) O. Jonas: Combined Cycle J. Second Quarter (2004) 1.